Design of PMaSynRM for Flywheel Energy Storage System in Smart Grids

Sadullah Esmer, Erdal Bekiroglu

Department of Electrical and Electronics Engineering, Bolu Abant Izzet Baysal University, 14280 Bolu, Turkey

(sadullahesmer@ibu.edu.tr, bekiroglu_e@ibu.edu.tr)

Corresponding Author; Erdal Bekiroglu, bekiroglu_e@ibu.edu.tr, Tel: +90 374 254 10 00/4872

Received: 14.11.2022 Accepted:21.12.2022

Abstract- In this study, a flywheel energy storage system (FESS) has been designed for smart grid applications. The requirements of the flywheel and electrical machine, which are the most important parts of FESS, have been determined. Analytical solutions approach has been performed for the flywheel with a capacity of 40 kWh. A high-speed permanent magnet-assisted synchronous reluctance machine (PMaSynRM) has been designed with Ansys Motor-Cad to meet the requirements of system. The torque-speed-power graph, thermal situation, magnetic flux lines, efficiency map, power map, and power factor map of FESS were analysed and obtained using the finite element method. Analyses were performed using Ansys Maxwell and the Machine Toolkit plugin. The results showed that the designed FESS offers high efficiency, high speed, and high energy storage capacity to be used in the smart grid applications.

Keywords: Smart grids, flywheel energy storage system (FESS), PMaSynRM, smart grid applications, synchronous reluctance machine.

1. Introduction

In the developing and changing world, the need for electrical energy is increasing day by day. There is a trend towards renewable energy sources, both to avoid the depletion of fossil fuel sources and to avoid harmful effects such as greenhouse gases [1]. It is important to obtain energy, it is also important to use and store energy efficiently. To meet these expectations, it is necessary to make electricity grids smarter. Smart grids are one of the topics that have gained importance recently. Smart grids allow efficient two-way communication with the electrical grid [2]. The general structure of smart grids is shown in Fig.1 [3]. Smart grids facilitate the use of renewable energy sources and contribute to environmentally friendly energy production. More efficient and widespread use of renewable energy sources can be achieved by improving integration with the grid and using energy storage systems [4]. For this purpose, there are applications such as distributed generation and distributed storage in smart grids [5]. Energy efficiency and reliability are very important in distributed generation. Smart grids should enable the integration of energy resources into the distribution grid in a wide range from small power generation to large power generation [6]. Thus, it will be possible to both produce and consume energy at the household level. This will transform the household that only consumes energy into a productive consumer. Distributed storage is an application that is used to meet the energy demand when necessary by storing the excess energy produced. Connecting the wide-scale energy storage system to the grid is important for more efficient use of energy-sustaining resources such as renewable energy [7].

There are many energy storage systems such as mechanical, chemical, electrochemical, electrical, and thermal [8], [9]. One of them is FESS. FESS is a mechanical energy storage system. Due to its advantages such as long lifetimes, high dynamics and good efficiencies, FESS is a suitable system for short-term energy storage [10]. Recently, studies on FESSs have increased. Some of these are related to the control of FESS [11], [12] and some studies are related to machine design [13-14]. There are many designs on FESS with different energy levels. In [15], the flywheel with a storage capacity of 5 kWh is designed. In [16], a flywheel that stores 8 kWh and can reach a speed of 18000 rpm has been designed. There are also studies about the flywheel, which can store 20 kWh and 0.5 kWh [17-18].

In this study, a 40kWh capacity FESS design to be used in smart grid applications has been presented. The aim of the study is to realize the design of a high energy storage capacity, high speed, and high efficiency FESS. Therefore, the size of

the flywheel and the required speed of the flywheel to store the targeted energy level were calculated. Considering requirements of FESS, the PMaSynRM was designed. Design and analyses of PMaSynRM were carried out in Ansys Motor-Cad and Ansys Maxwell. Torque-speed-power graph, thermal status, efficiency map, power map and power factor map of PMaSynRM were obtained and examined. It has been observed that the proposed FESS offers high energy storage capacity and high efficiency. The results showed that the designed FESS is valuable, applicable, and effective for smart grid applications.

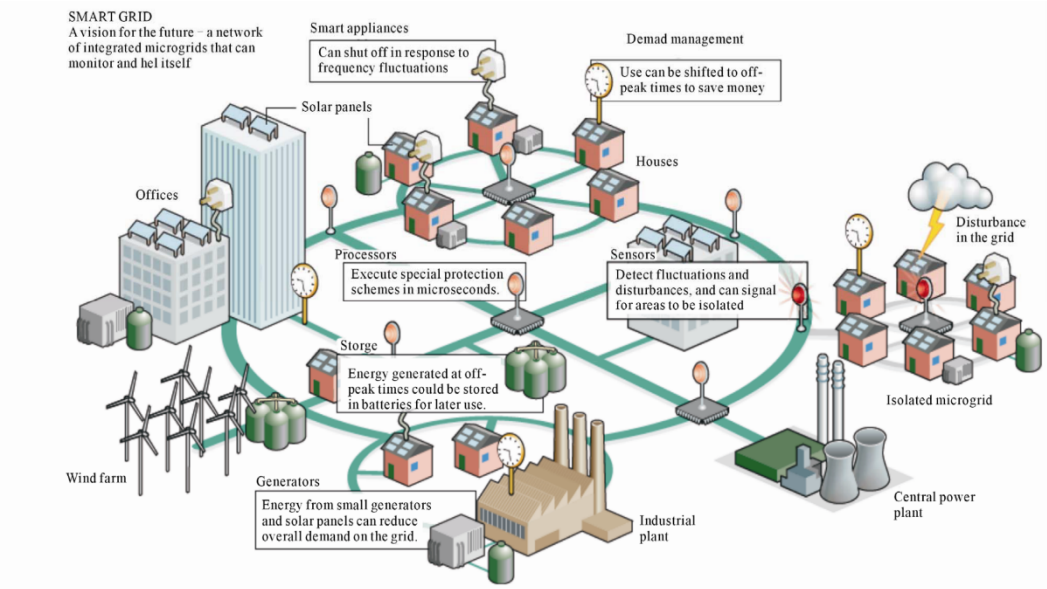

Fig. 1. A model of the smart grids.

2. Flywheel Energy Storage System (FESS)

FESSs are mechanical energy storage systems. In this system, there are flywheel, an electric machine that works as both motor and generator, bearings, and a driver [19]. FESS can be integrated into the grid together with the microgrid energy management system and power electronics controller. The structure of FESS is as shown in Fig. 2.

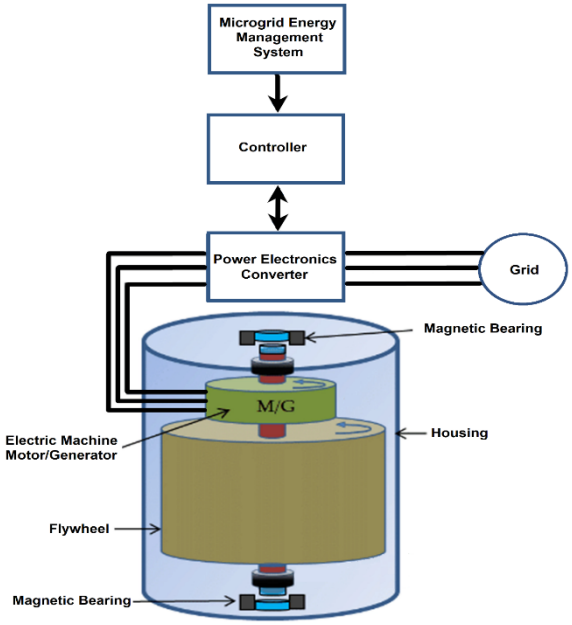

Fig. 2. The structure of FESS.

FESS stores mechanical energy by turning the flywheel. It is important to define the size of the flywheel because it determines the amount of energy to be stored.

2.1. Operating Principles of FESS

The energy stored in the system (E_{tot}) depends on the moment of inertia (J) and angular velocity (ω) of the flywheel as shown in Eq. (1).

$$E_{tot} = \frac{1}{2} J \omega^2 \tag{1}$$

The energy used or stored in FESS is directly related to the speed change of the flywheel. The change of energy is calculated as in Eq. (2).

$$E_{diff} = \frac{1}{2} J (\omega_{max}^2 - \omega_{min}^2 \tag{2}$$

The torque equation for the electric machine is shown in Eq. (3-4). Eq. (3) is motor mode and Eq. (4) is generator mode.

$$T_{em} = J \frac{d\omega}{dt} + B\omega + T_L \tag{3}$$

$$J \frac{d\omega}{dt} = T_{em} + B\omega + T_L \tag{4}$$

2.2. System Sizing and Design of Flywheel

FESS is required to store 40 kWh ($1.4 \times 10^8\, Joule$). Therefore, the rotation speed and inertia of the flywheel are

determined from Eq. (2). Considering similar studies in the literature, the minimum speed is determined for FESS [20]. This enables the control system of FESS to work more effectively. Therefore, the minimum speed for the targeted FESS has been determined. Eq. 5 is obtained from Eq. (4), considering the variable speeds of FESS and its losses due to changing speed.

$$\frac{1}{2}J(\omega_{max}^2 - \omega_{min}^2) = \int_{t1}^{t2} T_{em}\,\omega dt + \int_{t1}^{t2} B\omega^2\,dt \quad (5)$$

$$\frac{1}{2}J(\omega_{max}^2 - \omega_{min}^2) = \int_{t1}^{t2} T_{em}\,\omega dt + \int_{t1}^{t2} P_{fr}\,dt + \int_{t1}^{t2} P_{wind}\,dt \quad (6)$$

P_{fr} is mechanical friction loss and P_{wind} is wind loss in Eq. (6). Since magnetic bearings are used in the system, mechanical friction loss for the flywheel is neglected. Wind loss of the system has been calculated assuming that it operates at the environment values established in similar studies in the literature [20]. Wind loss (P_{wind}) of the system is calculated with the help of Eq. (7).

$$P_{wind} = \frac{1}{64} C_M \rho \omega^3 D_r^5 \quad (7)$$

$$C_M = \frac{3.87}{R_e{}^{0.5}} \quad (8)$$

$$R_e = \frac{\rho \omega D_r^2}{4\mu} \quad (9)$$

where C_M, ρ, D_r, R_e, and μ are torque coefficient, air density, flywheel diameter, Reynolds number and dynamic viscosity, respectively. The design parameters are given in Table 1. These parameters have been calculated analytically so that FESS store the desired amount of energy.

Table 1. Design parameters of FESS

Parameters	**Values**
Flywheel diameter ($D_{r)}$) (m)	1.53
Mass of flywheel (kg)	504.18
Material density (T100G/Epoxy) (gr/cm^3)	1.605
Moment of inertia (J) ($kg.m^2$)	149.1
Flywheel velocity (ω_{min}) (rad/s)/(rpm)	523/5000
Flywheel velocity (ω_{max}) (rad/s)/(rpm)	1486/14190
Used energy (E_{diff}) (Joule)	1.4×10^8
Dynamic viscosity (μ) (kg/m s)	1.9×10^{-5}
Air density (ρ) (kg/m^3)	5.6×10^{-3}
Torque coefficient (C_M)	0,007
Reynolds number (R_e)	2.6×10^5
Charge-discharge time (min)	140-60

The speed of the flywheel varies between the speeds given in Table 1. The energy that changes in these two speed ranges is the energy that the system can use. This is called a depth of discharge. The Depth of discharge (DD) shown in Eq. (10) was obtained from the velocity values in Table 1.

$$DD = 1 - \frac{\omega_{min}}{\omega_{max}} \approx 64.8\% \quad (10)$$

The efficiency for the flywheel designed using the design parameters in Table 1 can be calculated with the help of Eq. (1) and Eq. (7). The efficiency for the flywheel is shown in Eq. (11).

$$\eta = \frac{P_{tot} - P_{loss}}{P_{tot}} \quad (11)$$

Fig. 3 shows that an increase in the speed of the flywheel reduces the efficiency. As can be seen from Eq. (7), Increasing the speed of the flywheel increases the wind loss. Thus, efficiency of flywheel is lower at high speeds. The efficiency of the flywheel was observed to be the lowest 61.3% and the average 80%. The lowest efficiency was measured at the highest speed. A higher efficiency was obtained at lower speeds. In a review study, the efficiency of hybrid energy storage systems was examined. The efficiency of a system in which solar panels and Thermoelectric Generators are used is between 70% and 99.6%. If solar panels and diesel generators are used in the system, the efficiency is between 70% and 97% [21]. When the efficiency of these hybrid systems is examined, it is seen that FESS has a competitive efficiency. After determining the design parameters, electric machine requirements for FESS have been determined.

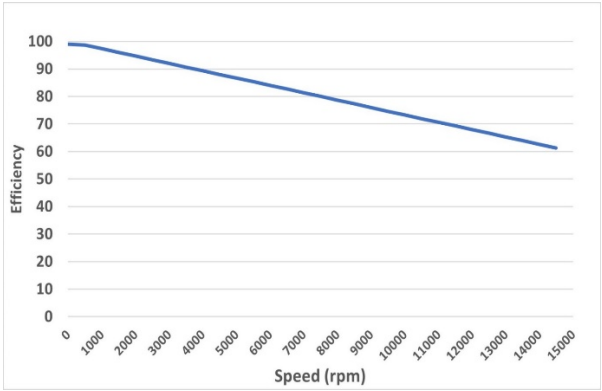

Fig. 3. Efficiency graph for flywheel.

2.3. Determining of Requirements for The Electric Machine

PMaSynRM to be used in FESS is designed to meet the maximum torque required by the system. To calculate maximum torque, the values of the flywheel at the highest speed were considered. The highest torque value required by the system is shown in Eq. (12).

$$T_{em} = T_{acc} + T_{wind} \quad (12)$$

T_{acc} is the acceleration torque, and T_{wind} is the torque required to overcome wind loss in Eq. (12). T_{acc} depends on the flywheel's moment of inertia (J) and speed variation. T_{wind} depends on wind loss at maximum speed. T_{acc} and T_{wind} are shown in Eq. (13-14), respectively. Equation (14) can be calculated by Eq. (7).

$$T_{acc} = J\frac{d\omega}{dt} \quad (13)$$

$$T_{wind} = \frac{P_{wind}}{\omega} \quad (14)$$

PMaSynRM increases the speed of the flywheel linearly from minimum to maximum in 140 minutes in motor mode. The required torque values are calculated using Table 1 and Eq. (13-14). Calculated torque values are given below.

$T_{acc} = 17.09\ Nm$

$T_{wind} = 11.65\ Nm$

$T_{em} = 28.74\ Nm$

PMaSynRM must produce 28.74 Nm of torque at 14190 rpm, which is the speed FESS needs to reach. PMaSynRM has been designed considering this situation.

3. Design and Analyses of PMaSynRM

PMaSynRM requirements for FESS were specified. Ansys Motor-Cad and Ansys Maxwell package programs were used for the design and analyses of the targeted PMaSynRM. Since PMaSynRM will work as both a motor and a generator, a magnet-assisted was preferred. There are many types of machines suitable for FESS in the literature. Some of those; Permanent magnet synchronous motor (PMSM), induction motor (IM) and switched reluctance motor (SRM) [22]. Since the electric machine in the FESS will be used as both a motor and a generator, a coiled or magnetized rotor will be advantageous. Wound rotor induction motor (WRIM) has a slip ring and brushes structure. Therefore, it has less reliability than permanent magnets motors at high speeds. Another type of IM is the squirrel-cage induction motor (SCIM). When the SCIM compared with PMaSynRM, it is seen that PMaSynRM has less losses and higher efficiency [23-25]. In a study, PMSM and PMaSynRM were compared. When the obtained results are examined, it is seen that PMaSynRM produces lower torque ripple, higher efficiency, lower back-EMF harmonics in the high-speed operating region [26]. In addition, because the magnets are embedded in the rotor of the PMaSynRM, it is more reliability at high speeds than motors with surface magnets. Comparison of PMaSynRM and other electrical machines is shown in Table 2 [27].

Table 2. Comparison of electric machines
(where "+" denotes advantages, " 0" for a neutral rating, "—" a disadvantages)

Criteria	Machine Type						
	DCM	IM	BLDC	PMSM	SRM	SynRM	PMaSynRM
Cost	0	++	-	-	+	++	+
Torque/power density	-	0	++	++	0	0	+
Efficiency	-	+	++	++	+	+	++
Controllability	++	+	+	+	0	+	+
Reliability	-	++	+	+	++	++	+
Size/weight/volume	-	+	++	++	+	+	+
Overload capability	-	+	+	+	+	++	++
Robustness	0	++	+	+	++	++	+
Field weakening	++	++	-	+	++	++	++
Fault tolerant	+	++	-	-	++	+	+
Thermal limitations	0	+	-	-	++	++	+
Noise/vibration/torque ripple	-	++	0	++	-	-	0
Lifetime	-	++	+	+	++	++	+
Future expectations	-	++	0	++	++	+	++

(DCM: DC Machine, BLDC: Brushless DC Machine, SynRM: Synchronous Reluctance machine)

As can be seen from Table 2, PMaSynRM has many advantages such as high efficiency, low cost, high reliability, and high fault tolerance. Therefore, PMaSynRM has been selected as the electric machine in the study.

PMaSynRM is designed in Motor-Cad to meet the specified requirements. The view of the designed PMaSynRM is given in Fig. 4.

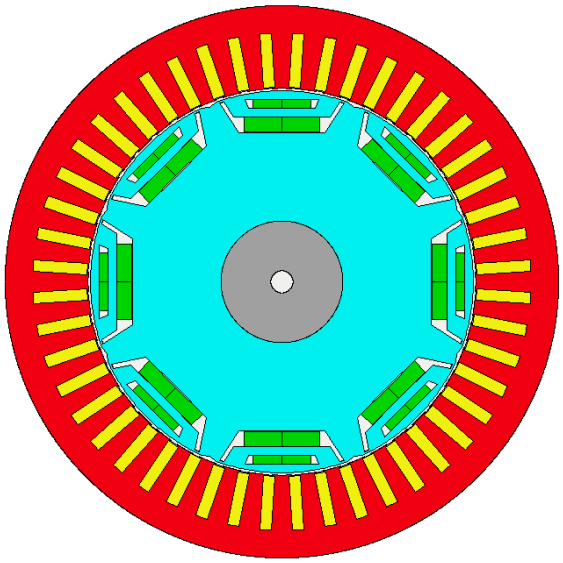

Fig. 4. 2D view of the designed PMaSynRM

Performance analysis of PMaSynRM was performed using the Ansys Maxwell Machine Toolkit plugin. The basic control system provided in Machine Toolkit was used to analysis the performance of PMaSynRM. The parameters used in the Machine Toolkit are given in Table 3 and the features of the designed PMaSynRM are given in Table 4. Torque-speed-power graph, thermal situation, efficiency map, power map, and power factor maps were obtained using Ansys Maxwell Machine Toolkit plugin.

Table 3. Parameters used in the Machine Toolkit

Parameters	**Values**
Machine Type	PM Synchronous
Number of Poles	8
Voltage Control	Sinusoidal PWM
Control Strategy	MTPA
Max RMS Line Current (A)	200
Max DC Voltage (V)	380
Maximum Speed (rpm)	14500

Table 4. Features of the designed PMaSynRM

Parameters	**Values**	**Parameters**	**Values**
Number of slots	48	Peak Torque (Nm)	296.9
Number of poles	8	Maximum speed (rpm)	14500
Number of phases	3	Desired speed (rpm)	14190
Voltage (V)	380	Torque (Nm) @Desired speed	29
Maximum current rms (A)	185	Power (kW) @Desired speed	42.4
Peak power (kW)	56	Peak efficiency (%)	94

Magnetic analyses were carried out using the finite element method. With the help of these analyses, a torque-speed-power graph was obtained. This graph is shown in Fig. 5. When the graph is examined, it is seen that the PMaSynRM produces between 22 and 296.9 Nm of torque and offers an operating range up to 14500 rpm. PMaSynRM also provides a peak power of 56 kW. It was calculated that the PMaSynRM should provide 28.74 Nm of torque at 14190 rpm for the purposed FESS. It is seen that the designed PMaSynRM fulfills this requirement.

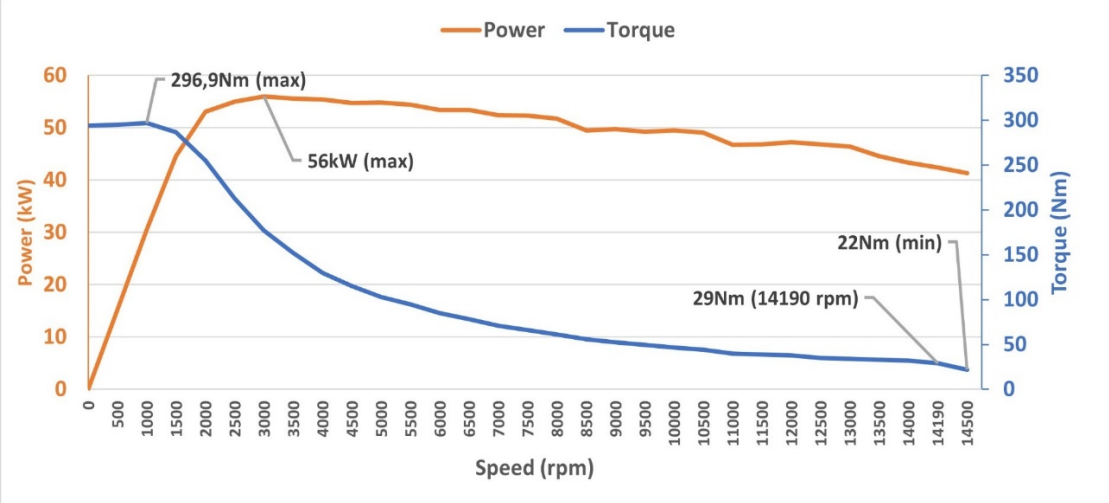

Fig. 5. Torque-speed-power graph of the designed PMaSynRM

The thermal analysis and magnetic analysis of PMaSynRM are also shown in Fig. 6. When the thermal situation of the PMaSynRM is analysed, it is seen that the highest temperature (90.8ºC) occurs in the windings. Since the magnet type N42UH used in SynRM can be used above 100ºC, the measured temperature of SynRM is an acceptable value [28]. Magnetic flux lines of 8 pole PMaSynRM are also seen in Fig. 6.

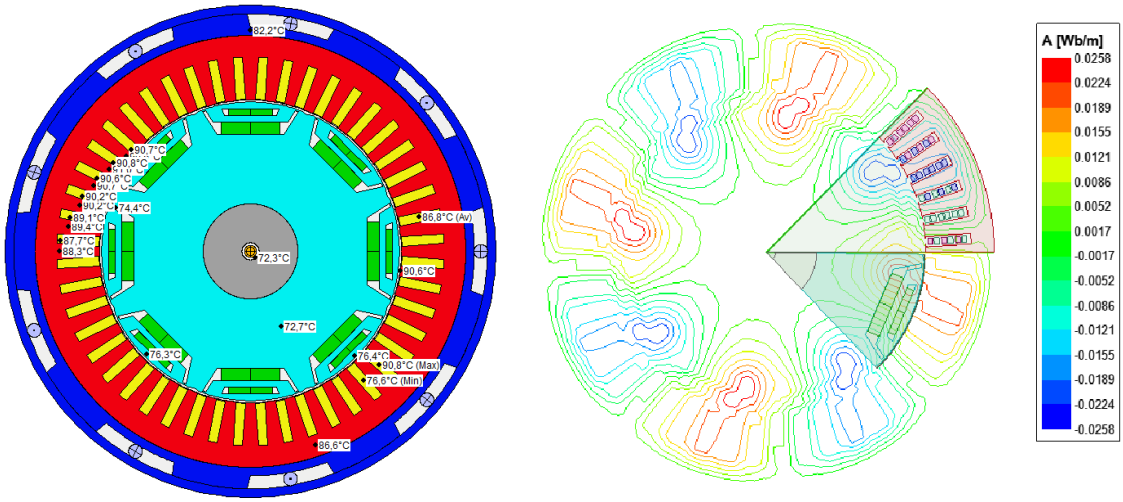

Fig. 6. Thermal and magnetic analyses of the designed PMaSynRM

The efficiency map shows how efficient a machine is along the torque and speed axes. It is desirable that the efficiency is high, but the efficiency decreases as the losses increase. The efficiency map of the PMaSynRM is shown in Fig. 7. The highest efficiency of PMaSynRM is 94%. Throughout FESS's operation, the efficiency of PMaSynRM varies between 75% and 94%. In this process, the average efficiency of PMaSynRM was measured as 84%.

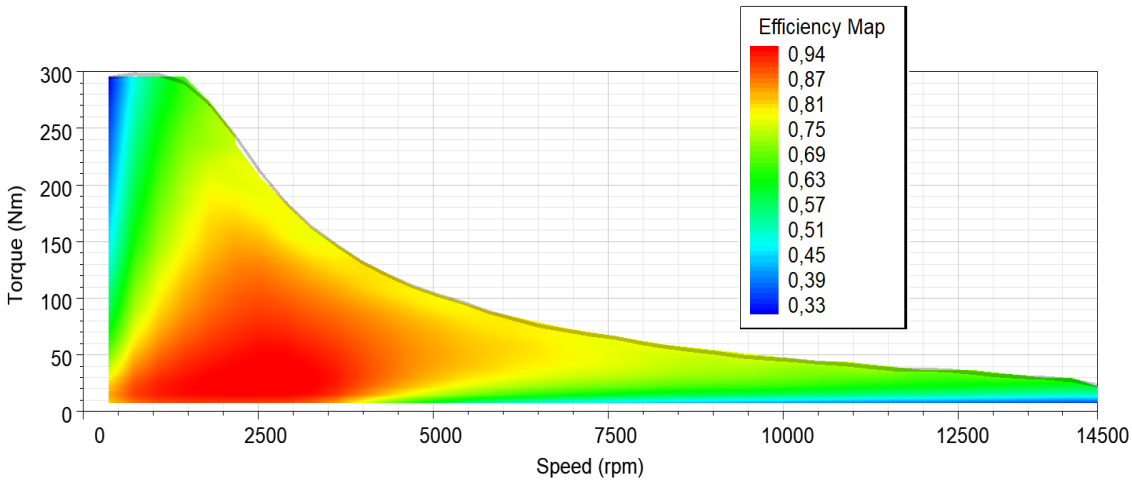

Fig. 7. Efficiency map of the designed PMaSynRM

The power map and power factor map of the PMaSynRM were also obtained with magnetic analyses. The power map shows the instantaneous power of an electric machine in the torque and speed axes. The power map of PMaSynRM is shown in Fig. 8. The torque of the PMaSynRM is directly related to its output power. Higher torque is achieved at higher output power in a speed range. The highest output power of PMaSynRM is approximately 56 kW. Fig. 9 shows the power factor map of PMaSynRM. The power factor shows how efficiently electrical energy is used by electric machine. The designed PMaSynRM has a power factor greater than 0.9 over a wide range. Consequently, the high-power factor of PMaSynRM enables the designed FESS to operate more efficiently.

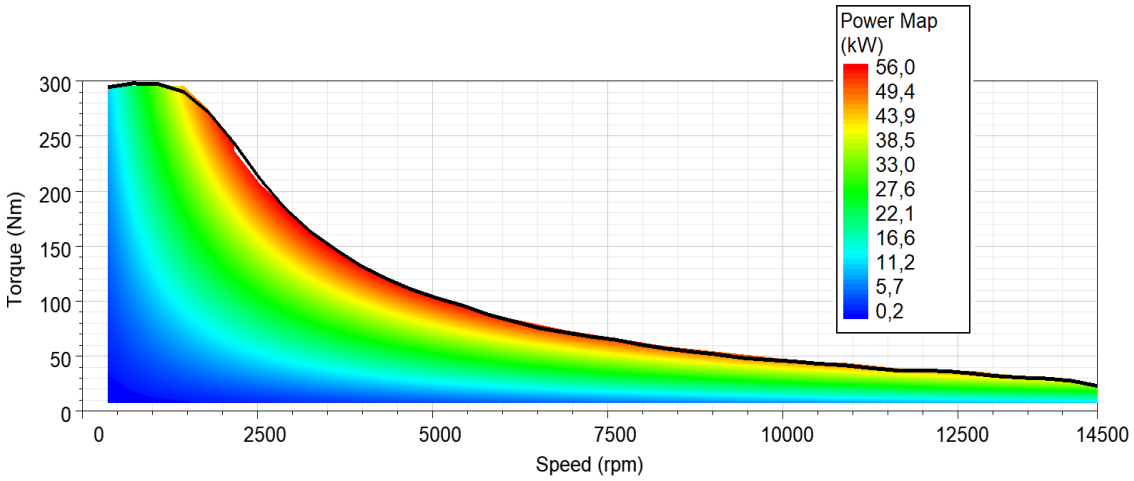

Fig. 8. Power map of the designed PMaSynRM

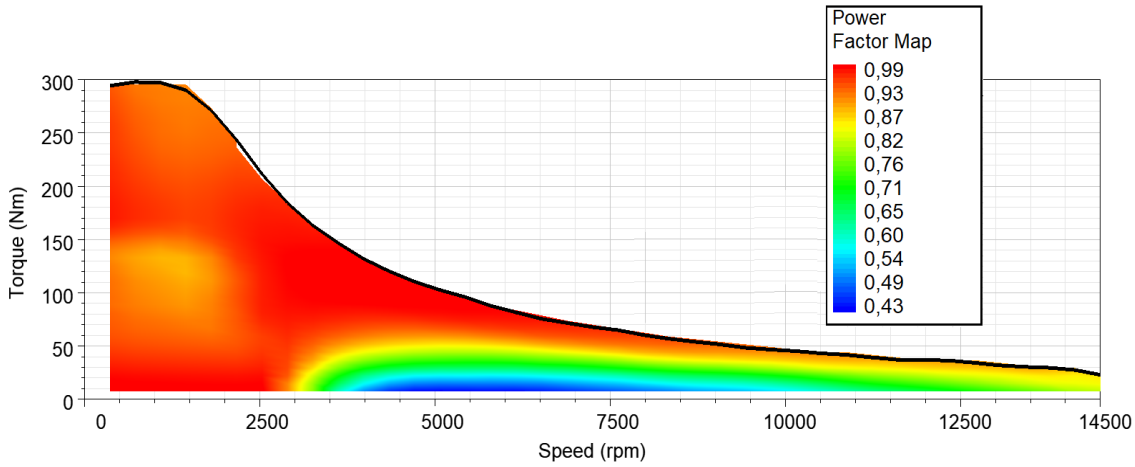

Fig. 9. Power factor map of the designed PMaSynRM

The analyses results show that the designed PMaSynRM meets the targeted requirements. It has been revealed that this study offers a higher level of energy storage while compared with the studies presented in the literature [12-15, 18].

4. Conclusion

This paper presents a design for an energy storage application, which is part of the smart grid applications. In the study, a flywheel energy storage system (FESS) which is a mechanical energy storage system was designed. The parameters of the flywheel have been calculated analytically to provide 40 kWh energy store capacity. As a result of the calculations, the maximum speed and required torque of the flywheel were determined to store the targeted energy level. PMaSynRM was preferred for an electrical machine that would meet the specified requirements. PMaSynRM has high efficiency, high reliability, and good torque/power density. There are electrical machines with higher torque/power density, but there is a tradeoff relationship when cost and efficiency are considered. The rotor of the PMaSynRM has cavities that feature flux barriers. Therefore, it is difficult to manufacture the rotor. However, these cavities provide the advantage of lower inertia as they reduce the weight of the rotor. The design and analyses of PMaSynRM was realized in Ansys Motor-Cad and Ansys Maxwell programs. Analyses were carried out using the finite element method. Thermal status, torque-speed-power graph, efficiency map, power map and power factor map of PMaSynRM were obtained. According to the analytical solution and simulation results, the efficiency of the flywheel was observed to be the lowest 61.3% and average 80% while the efficiency of the PMaSynRM was observed to be the highest 94% and average 84%. When the results are examined, it is seen that a FESS model has been created that offers high efficiency, high speed, and high energy storage.

References

[1] M. Akil, E. Dokur, and R. Bayindir, “A Coordinated EV Charging Scheduling Containing PV System,” International Journal of Smart Grid, vol. 6, no. 3, pp. 65–71, 2022.

[2] B. Kocaman, “Akıllı Şebekeler ve Mikro Şebekelerde Enerji Depolama Teknolojileri,” Bitlis Eren Üniversitesi Fen Bilimleri Dergisi, vol. 2, no. 1, pp. 119–127, 2013.

[3] T. Vijayapriya and D. Pralhadas Kothari, “Smart Grid: An Overview,” Smart Grid Renew. Energy, vol. 2, pp. 305–311, 2011.

[4] J. M. Guerrero, L. García de Vicuña, and M. Castilla, "Hierarchical Control of Droop-Controlled AC and DC Microgrids—A General Approach Toward Standardization," IEEE Trans. Ind. Electron., vol. 58, no. 1, pp. 158–172, 2011.

[5] S. N. Saxena, "Trilemma of Smart Distribution Grid: People, Processes and Environment," International Journal of Smart Grid, vol. 4, no. 1, 2020.

[6] B. B. Alagoz, A. Kaygusuz, and A. Karabiber, "A user-mode distributed energy management architecture for smart grid applications," Energy, vol. 44, no. 1, pp. 167–177, 2012.

[7] A. Oymak and M. R. Tür, "A Short Review on the Optimization Methods Using for Distributed Generation Planning," International Journal of Smart Grid, vol. 6, no. 3, pp. 54–64, 2022.

[8] A. R. Dehghani-Sanij, E. Tharumalingam, M. B. Dusseault, and R. Fraser, "Study of energy storage systems and environmental challenges of batteries," Renew. Sustain. Energy Rev., vol. 104, pp. 192–208, Apr. 2019.

[9] A. Belkaid, I. Colak, K. Kayisli, and R. Bayindir, "Modeling of a Permanent Magnet Synchronous Generator in a Power Wind Generation System with an Electrochemical Energy Storage," International Journal of Smart Grid, vol. 2, no. 4, 2018.

[10] M. Subkhan and M. Komori, "New concept for flywheel energy storage system using SMB and PMB," IEEE Trans. Appl. Supercond., vol. 21, no. 3, pp. 1485–1488, Jun. 2011.

[11] M. Shadnam Zarbil, A. Vahedi, H. Azizi Moghaddam, and M. Saeidi, "Design and implementation of flywheel energy storage system control with the ability to withstand measurement error," J. Energy Storage, vol. 33, p. 102047, Jan. 2021.

[12] H. Gao, W. Li, and H. Cai, "Distributed control of a flywheel energy storage system subject to unreliable communication network," Energy Reports, vol. 8, pp. 11729–11739, Nov. 2022.

[13] J. Yang, P. Liu, C. Ye, L. Wang, X. Zhang, and S. Huang, "Multidisciplinary Design of High-Speed Solid Rotor Homopolar Inductor Machine for Flywheel Energy Storage System," IEEE Transactions on Transportation Electrification, vol. 7, no. 2, pp. 485–496, Jun. 2021.

[14] Z. Q. Liu, K. Wang, and F. Li, "Design and Analysis of Permanent Magnet Homopolar Machine for Flywheel Energy Storage System," IEEE Transactions on Magnetics, vol. 55, no. 7, Jul. 2019.

[15] P. Haidl and A. Buchroithner, "Design of a Low-Loss, Low-Cost Rolling Element Bearing System for a 5 kWh/100 kW Flywheel Energy Storage System," Energies, vol. 14, no. 21, p. 7195, 2021.

[16] A. Floris, A. Damiano, and A. Serpi, "Design and performance assessment of an integrated flywheel energy storage systems based on an inner-rotor large-airgap SPM," Proc. - 2020 Int. Conf. Electr. Mach. ICEM 2020, pp. 633–639, Aug. 2020.

[17] J. Gao, S. Zhao, J. Liu, W. Du, Z. Zheng, and F. Jiang, "A novel flywheel energy storage system: Based on the barrel type with dual hubs combined flywheel driven by switched flux permanent magnet motor," J. Energy Storage, vol. 47, p. 103604, Mar. 2022.

[18] X. Li, D. Dietz, J. An, N. Erd, Y. Gemeinder, and A. Binder, "Manufacture and Testing of a Magnetically Suspended 0.5 kWh-Flywheel Energy Storage System," IEEE Transactions on Industry Applications, 2022.

[19] M. M. Biswas et al., "Towards Implementation of Smart Grid: An Updated Review on Electrical Energy Storage Systems," Smart Grid Renew. Energy, vol. 4, no. 1, pp. 122–132, 2013.

[20] K. AYDIN and M. T. AYDEMİR, "Sizing design and implementation of a flywheel energy storage system for space applications," Turkish Journal of Electrical Engineering & Computer Sciences, vol. 24, no. 3, pp. 793–806, 2016.

[21] K. Kayisli, R. zafer Caglayan, N. Zhakiyev, A. Harrouz, and I. Colak, "A Review of Hybrid Renewable Energy Systems and MPPT Methods," International Journal of Smart Grid, vol. 6, no. 3, pp. 72–78, 2022.

[22] X. Li and A. Palazzolo, "A review of flywheel energy storage systems: state of the art and opportunities," J. Energy Storage, vol. 46, p. 103576, 2022.

[23] R. Vartanian and H. A. Toliyat, "Design and comparison of an optimized permanent magnet-assisted synchronous reluctance motor (PMa-SynRM) with an induction motor with identical NEMA frame stators," IEEE Electric Ship Technologies Symposium 2009, pp. 107–112, 2009.

[24] H. Kim, Y. Park, H. C. Liu, P. W. Han, and J. Lee, "Study on Line-Start Permanent Magnet Assistance Synchronous Reluctance Motor for Improving Efficiency and Power Factor," Energies 2020, Vol. 13, Page 384, vol. 13, no. 2, p. 384, Jan. 2020.

[25] S. Jia, P. Zhang, D. Liang, M. Dai, and J. Liu, "Design and Comparison of Three Different Types of IE4 Efficiency Machines," International Conference on Electrical Machines and Systems, 2019.

[26] Y. H. Jeong, K. Kim, Y. J. Kim, B. S. Park, and S. Y. Jung, "Design characteristics of PMa-SynRM and performance comparison with IPMSM based on numerical analysis," International Conference on Electrical Machines, pp. 164–170, 2012.

[27] M. Yilmaz, "Limitations/capabilities of electric machine technologies and modeling approaches for electric motor design and analysis in plug-in electric vehicle applications," Renewable and Sustainable Energy Reviews, vol. 52, pp. 80–99, 2015.

[28] H. Huang, L. Jing, R. Qu, and D. Li, "The Demagnetizing Protection of Halbach Consequent Pole in a Magnetic-Geared Machine," International Conference on Electrical Machines and Systems, pp. 365–370, Nov. 2018.